Noninvasive Measurements of [1-^{13}C]Glycogen Concentrations and Metabolism in Rat Brain In Vivo

In-Young Choi, Ivan Tkáč, Kâmil Uğurbil, and Rolf Gruetter

Department of Radiology, Center for MR Research, University of Minnesota, Minneapolis, Minnesota, U.S.A.

Abstract: Using a specific ^{13}C NMR localization method, ^{13}C label incorporation into the glycogen C1 resonance was measured while infusing [1-^{13}C]glucose in intact rats. The maximal concentration of [1-^{13}C]glycogen was 5.1 $\pm$ 0.6 μmol g^{-1} (mean $\pm$ SE, n = 8). During the first 60 min of acute hyperglycemia, the rate of ^{13}C label incorporation (synthase flux) was 2.3 $\pm$ 0.7 μmol g^{-1} h^{-1} (mean $\pm$ SE, n = 9 rats), which was higher ($p < 0.01$) than the rate of 0.49 $\pm$ 0.14 μmol g^{-1} h^{-1} measured $\geq$2 h later. To assess whether the incorporation of ^{13}C label was due to turnover or net synthesis, the infusion was continued in seven rats with unlabeled glucose. The rate of ^{13}C label decline (phosphorylase flux) was lower (0.33 $\pm$ 0.10 μmol g^{-1} h^{-1}) than the initial rate of label incorporation ($p < 0.01$) and appeared to be independent of the duration of the preceding infusion of [1-^{13}C]glucose ($p > 0.05$ for correlation). The results implied that net glycogen synthesis of ~3 μmol g^{-1} had occurred, similar to previous reports. When infusing unlabeled glucose before [1-^{13}C]glucose in three studies, the rate of glycogen C1 accumulation was 0.46 $\pm$ 0.08 μmol g^{-1} h^{-1}. The results suggest that steady-state glycogen turnover rates during hyperglycemia are ~1% of glucose consumption. **Key Words:** NMR—Glucose transport—In vivo studies—Spectroscopy—Glycogen phosphorylase—Glycogen synthase.
J. Neurochem. **73,** 1300–1308 (1999).

It is well known that the brain is almost exclusively dependent on blood glucose as the major source for ATP synthesis in the brain (Siesjö, 1978). The brain maintains a small glycogen reserve on the order of a few micromoles per gram, which provides the energy for a few minutes of complete ischemia (Lowry et al., 1964; Swanson et al., 1989; Folbergrová et al., 1996). The small cerebral glycogen concentration of 2–5 μmol g^{-1} glucosyl units reported in rodents (Nelson et al., 1968; Strang and Bachelard, 1971; Sagar et al., 1987; Garriga and Cusso, 1992) makes biochemical measurements rather difficult. A previous study found that 2% of total tissue radioactivity was detected in extracted glycogen 45 min after pulsed administration of the 2-deoxyglucose (Nelson et al., 1984). Studies have suggested that brain glycogen has an active metabolism that can be affected by neuronal activity (Swanson, 1992), as well as by

hormones (Meguid et al., 1993) and several neurotransmitters (Magistretti et al., 1986; Sorg and Magistretti, 1992). Recent studies using quantitative autoradiography have shown that focal physiologic stimulation may lead to cerebral glycogen breakdown (Swanson et al., 1992). Global ischemia results in rapid glycogenolysis with near complete depletion in a few minutes (Lowry et al., 1964; Swanson et al., 1989; Folbergrová et al., 1996). Early studies have suggested that brain glycogen can be modulated by hyperglycemia, barbiturate anesthesia, and hyperinsulinemia (Nelson et al., 1968). In summary, substantial evidence suggests that brain glycogen metabolism may be controlled by several factors that may have complex interactions (for review, see, e.g., Swanson, 1992).

Brain glycogen was shown in adult nervous tissue to be localized to the glial compartment by many studies (see, e.g., Wiesinger et al., 1997, and references therein), and glycogen phosphorylase was shown to be exclusively localized to glial cells (Pfeiffer et al., 1992). Recent studies have shown a much higher similarity of the genes expressing glycogen synthase (Pellegri et al., 1996) and phosphorylase (Newgard et al., 1988) to the genes expressing the corresponding isoenzymes in the muscle than to the corresponding genes expressing the liver isoenzymes. The structure of brain glycogen thus is probably similar to that of muscle glycogen, which was supported by structural studies (Chee et al., 1983).

To date, all methods used to assess brain glycogen metabolism depend either on biochemical analysis or on autoradiography of brain slices or on culture studies. The limitations imposed by the rapid agonal changes in brain glycogen content have been documented in the literature,

and these limitations have been minimized to some extent using optimized extraction procedures, of which microwave fixation reported the highest concentration (Strang and Bachelard, 1971; Sagar et al., 1987; Garriga and Cusso, 1992). As an alternative, glycogen metabolism has been studied in astrocyte cultures (Wiesinger et al., 1997, and references therein), but these model systems may not completely mimic the coupling of energy metabolism between glia and neurons in vivo. Direct in vivo measurement of brain glycogen is expected to provide further insight into the role glycogen plays in brain metabolism. Of particular interest are noninvasive studies of glycogen in the human brain, of which very little is known.

The glycogen C1 resonance can be reliably measured noninvasively using natural abundance ^{13}C NMR (Gruetter et al., 1991, 1994a; Taylor et al., 1992) in the liver—where the glycogen concentration is on the order of 100–500 $\mu mol\ g^{-1}$—and in the muscle—with a concentration of 30–100 $\mu mol\ g^{-1}$ (for review, see Shulman et al., 1995). In contrast, the brain glycogen concentration is one to two orders of magnitude lower, which is difficult to detect using natural-abundance ^{13}C NMR. In *all* ^{13}C NMR studies of glycogen in the literature, full three-dimensional localization has not been reported to date. As an alternative, ^1H NMR can potentially be used to detect glycogen in vivo (Chen et al., 1994). A recent report suggested that brain glycogen may be observable in patients with McArdle's disease (Salvan et al., 1997). In a preliminary report we have shown that a distinct, weak resonance at 5.35 ppm was observed in ^1H NMR spectra from a rat brain in vivo when using an echo time of 1 ms, tentatively assigned to glycogen or potentially overlapping free fatty acid signal (Tkac et al., 1999), corresponding to a signal on the order of 1 $\mu mol\ g^{-1}$, suggesting a low visibility in vivo.

According to the aforementioned studies measuring radiolabel incorporation into brain glycogen, it should be possible to enhance the sensitivity of ^{13}C NMR by observing ^{13}C label transfer into the small brain glycogen pool with ^{13}C-labeled glucose infusions. A completely nondestructive approach required the elimination of the signal from ~10-fold more concentrated muscle glycogen present in superficial muscle tissue, which may overwhelm the cerebral glycogen NMR signal. To overcome this limitation, we specifically developed and optimized a localization method suitable for brain glycogen detection. To assess further whether the observed label incorporation into brain glycogen reflects mostly isotope exchange (turnover) or net synthesis, the change in [1-^{13}C]glycogen was measured by switching the infusate to unlabeled glucose (pulse–chase experiment) and by reversing the order of label in the infusion (unlabeled glucose followed by [^{13}C]glucose). The purpose of this study was (a) to evaluate whether ^{13}C NMR can provide a completely noninvasive measurement of brain glycogen C1 signal, (b) to test under what circumstances ^{13}C NMR detection of brain glycogen metabolism is possible

in vivo, and (c) to attempt to characterize further in vivo brain glycogen turnover.

MATERIALS AND METHODS

Animals

Fifteen male Sprague–Dawley rats (weighing 245 ± 12 g, mean ± SE) were anesthetized with intravenous α-chloralose administration with an initial dose of 40 mg/kg in the first hour and a continuous infusion of 13.2 mg $kg^{-1}\ h^{-1}$ thereafter. Rats were ventilated at physiological conditions with a gas mixture of 60%/40% O_2/N_2O after intubation. Arterial pH was maintained between 7.2 and 7.4 (7.35 ± 0.02, mean ± SE), and arterial blood pressure and respiratory pressure were recorded during the entire experimental time using AcqKnowledge (Biopac Co., Santa Barbara, CA, U.S.A.). P_{aO_2} was maintained between 144 and 164 mm Hg and, likewise, P_{aCO_2} was maintained between 32 and 48 mm Hg (37 ± 1.7 mm Hg). Oxygen saturation was maintained >95% and continuously monitored with an infrared sensor clipped to the tail (Nonin Medical, Minneapolis, MN, U.S.A.). A rectal thermosensor (Cole-Parmer, Vernon Hills, IL, U.S.A.) was used to verify that the body temperature was at 37°C, which was maintained by placing the rats on a heated water blanket.

A femoral venous line was used for infusion of a 20% (wt/vol) solution of D-[1-^{13}C]glucose (Isotec, Miamisburg, OH, U.S.A.), prepared as 70 or 100% ^{13}C-enriched. To achieve rapid ^{13}C enrichment of plasma glucose, [1-^{13}C]glucose was administered according to previously published procedures (Patlak and Pettigrew, 1976; Fitzpatrick et al., 1990; Terpstra et al., 1998). The glucose infusion protocol was always as follows: A bolus of 0.8 mg (g wet wt)$^{-1}$ was administered in 1 ml in the first 5 min, followed by a glucose infusion at 0.065 mg min^{-1} (g wet wt)$^{-1}$ rat for 20 min, which was dropped to 0.04 mg min^{-1} (g wet wt)$^{-1}$ for the next 20 min, and then maintained at 0.03 mg min^{-1} (g wet wt)$^{-1}$ thereafter. The initial glucose administration was very similar to the one used previously, which we verified to yield modestly elevated, stable arterial plasma glucose concentrations between 13 and 16 mM, as illustrated by Terpstra et al. (1998). Similar infusion protocols adapted to humans have been shown to produce rapid, stable brain glucose ^{13}C enrichment (Gruetter et al., 1994b, 1998a). The infusion protocol was used irrespective of the presence of ^{13}C label in the infused glucose solution.

Infusions of glucose were started 3 h after preparation of the animals.

In vivo NMR methods

The NMR instrumentation was a Varian (Palo Alto, CA, U.S.A.) INOVA spectrometer interfaced to a 31-cm horizontal bore, 9.4-T magnet with an 11-cm actively shielded gradient capable of switching 300 mT/m in 500 μs (Magnex Scientific, Abingdon, U.K.). A quadrature 400-MHz ^1H surface radiofrequency coil (14 mm in diameter, distributed capacitance) combined with a linearly polarized, triple-turn 100-MHz ^{13}C coil with a diameter of 12 mm was used (Adriany and Gruetter, 1997). Shimming of all first- and second-order shim coils was done with FASTMAP (Gruetter, 1993; Gruetter et al., 1998b), typically resulting in 18–26 Hz linewidth of the water resonance in a $9 \times 5.5 \times 12\ mm^3$ voxel (~600 μl), which was located on the midline and 1.5 mm posterior to the bregma. Processing of ^{13}C NMR spectra consisted of exponential multiplication (corresponding to a line broadening of 30 Hz), fast Fourier transformation, baseline correction, and integration, all of which were performed using built-in spectrometer software.

With these processing parameters, the brain glycogen linewidth was 87 ± 10 Hz (mean $\pm$ SD), which did not vary >10% throughout each experiment.

To minimize contamination due to much more concentrated glycogen in superficial muscle, we used outer volume suppression similar to previous reports (Shungu and Glickson, 1993; Luo et al., 1995; Chen et al., 1997). The outer volume suppression pulses were a series of pulses of the hyperbolic secant type (Tannus and Garwood, 1996) 2–8 ms in duration, used as either (nonadiabatic) ~90° pulses or adiabatic 180° pulses with timing adjusted to minimize the glycogen signal in six slices surrounding the volume of interest. In addition, an alternating 180° pulse with concomitant phase cycling (Ordidge et al., 1986) was applied to localize the slice parallel to the carbon surface coil. The excitation pulse was a 400-μs half-passage pulse with tanh/tan modulation applied at 100.5 ppm, and the detection frequency was placed between the signal of glycogen C1 and the C1 of β-glucose.

Performance of the NMR pulse sequence used for localization of glycogen signals was validated in two-compartment phantoms consisting of a cylindrical tube 14 mm in diameter containing a concentrated solution of glucose or myo-inositol placed into a 24-mm-diameter cylindrical tube containing a 400 mM natural abundance oyster glycogen solution. The power of the outer volume suppression pulses was calibrated relative to the power needed to invert the ^{13}C-labeled formic acid signal from an external reference sphere placed at the ^{13}C coil center. WALTZ-16 decoupling (Shaka et al., 1983) in the proton channel was applied during the entire acquisition time of 90 ms, and decoupling power was <3 W. The decoupler was gated to 0.1 W for generation of a nuclear Overhauser effect during the recovery delay; the repetition time (TR) was 600 ms. A temporal resolution of 1.5 or 3 min resulted from collecting the data in either 128 or 256 scans per block, respectively, which includes delays incurred from storing the data to disk. For some of the data analysis, signal-to-noise was improved by coadding the individual spectra.

Quantification of ^{13}C-labeled glycogen C1 resonance

The ^{13}C-labeled glycogen C1 resonance was quantified using the external reference method as in previous ^{13}C magnetic resonance spectroscopy measurements of muscle glycogen C1 in vivo (Gruetter et al., 1991; Taylor et al., 1992). This method uses the comparison with an identical experiment performed on a phantom solution of the same metabolite, which can be used to calibrate the in vivo signal after suitable corrections for loading. In brief, the effect of variable coil loading on sensitivity was assessed by measuring the signal of the sphere placed at the ^{13}C coil center containing an aqueous solution of ^{13}C-labeled formic acid. In addition, the duration of a rectangular 180° pulse applied to the formic acid signal was measured, which provided an independent assessment of coil loading effects. Both measurements of coil loading effects on sensitivity were within 15% of each other. The [1-^{13}C]glycogen signal was quantified by performing the identical experiment on a phantom containing ~400 mM natural abundance oyster glycogen ([Glyc]$_o$), taking into account the 1.1% natural abundance of ^{13}C. The external reference method for quantification of the glycogen C1 signal was based on the following equation, as in previous studies (Gruetter et al., 1991, 1994a; Taylor et al., 1992):

$$[\text{Glyc}] = \frac{I_{\text{Glyc}}^{\text{in vivo}} \cdot I_{\text{FA}}^{\text{ref}} \cdot [\text{Glyc}]_o \cdot 0.011}{I_{\text{Glyc}}^{\text{ref}} \cdot I_{\text{FA}}^{\text{in vivo}}} \qquad (1)$$

where I_{Glyc} denotes the integrated NMR signal of glycogen, and I_{FA} denotes that of formic acid measured from the phantom reference experiment (ref) or measured from the rat brain (in vivo). In one rat, the concentration was obtained by dividing the [^{13}C]glycogen signal by 0.7 to account for the lower enrichment of 70% used for the [^{13}C]glucose infusion. Equation 1 assumes that the saturation factors of glycogen are identical in vivo and in solution, which was supported by the observation that the T_1 of in vivo glycogen was within 10% of that measured from oyster glycogen solutions and that the repetition time used for the quantification was approximately two times T_1. The inversion recovery method was used to assess T_1 for in vivo glycogen in two rats, which was found to be 0.31 ± 0.01 s, and that for oyster glycogen was found to be 0.34 ± 0.02 s, both of which are in excellent agreement with previous reports (Zang et al., 1990; Overloop et al., 1996).

Assessment of rate of ^{13}C incorporation into glycogen C1

Changes in glycogen C1 signal were assessed by the slope of a linear regression of data points measured over a contiguous 60-min period. For these assessments, we pooled the time-resolved data into 6-min spectra, which provided 10 time points per slope determination. The median time was assigned to such a measurement; hence, the synthase flux, V_{syn} (rate of [1-^{13}C]-glycogen accumulation), measurement indicated with V_{syn} ($t = 30$) represents the slope measured over $t = 0$–60 min, V_{syn} ($t = 90$) represents the slope measured from 60 to 120 min, etc. The nine experiments resulted in nine measurements of the rate of glycogen C1 increase at $t = 30$ after the start of [^{13}C]glucose administration. Because the slopes measured at $t > 150$ min appeared to be independent of t (correlation coefficient $r = -0.04$; $p > 0.05$), we averaged all 24 slope measurements starting at 120 min, resulting in one rate value, denoted V_{syn} ($t > 150$).

When assuming that label incorporation into plasma glucose is rapid compared with synthase flux, V_{syn}, and phosphorylase flux, V_{phos} (rate of [1-^{13}C]glycogen breakdown during unlabeled glucose infusions), and that turnover is the sole mechanism by which label is incorporated into glycogen, the initial rate of glycogen accumulation will be approximated by

$$\frac{d^{13}\text{Glyc}_1(t)}{dt} \approx V_{\text{syn}} \qquad (2)$$

which slightly underestimates V_{syn}. Conversely, when changing the label from [1-^{13}C]glucose to natural abundance glucose and assuming that the ^{13}C-labeled glucose is reduced to natural abundance in a short time compared with V_{phos}, the initial rate of glycogen signal decrease is given by

$$\frac{d^{13}\text{Glyc}_1(t)}{dt} \approx -V_{\text{phos}} \qquad (3)$$

This approximation underestimates the true V_{phos}, if elimination of ^{13}C label is not fast. For example, after 2 h, labeled glucose was not further detectable, and a [1-^{13}C]glycogen concentration decrease of ~20% of the maximum was observed (see Results). In this case, the rate of [1-^{13}C]glycogen decrease is given by

$$\frac{d^{13}\text{Glyc}_1(t)}{dt} \approx -0.8 \, V_{\text{phos}} \qquad (4)$$

i.e., the rates of brain glycogen degradation reported underestimate the flux through glycogen phosphorylase in vivo by 25%.
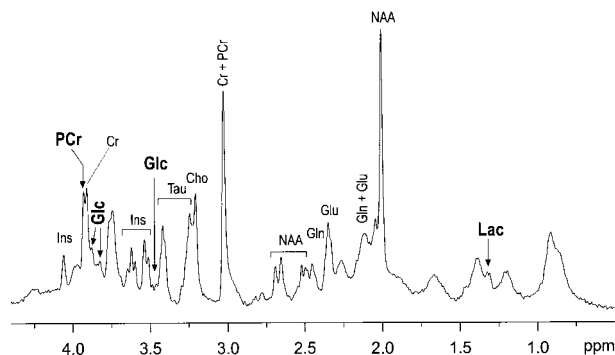
FIG. 1. ^{1}H NMR spectroscopy of rat brain. The ^{1}H NMR spectrum was acquired as described elsewhere (Tkac et al., 1999). In brief, a stimulated echo sequence with a seven-pulse water suppression scheme was used (2-ms echo time, 5-ms mixing time, 4-s repetition time, 320 scans, 100-μl volume). Processing consisted of moderate Gaussian resolution enhancement and fast Fourier transformation. Resonances from phosphocreatine (PCr; arrow), glucose (Glc; arrow), and lactate (Lac; arrow) were discernible among resonances from *myo*-inositol (Ins), taurine (Tau), choline (Cho), creatine (Cr), glutamate (Glu), glutamine (Gln), and *N*-acetylaspartate (NAA). PCr was within normal limits, and the low Lac signal of ~10% of NAA implied a normal brain Lac concentration of ~1 μmol g^{-1}.

For statistical tests, the two-tailed *t* test and Pearson's rank correlation test were used, where appropriate.

RESULTS

Throughout the study, physiological stability of the rats was regularly monitored. As judged from the excellent T_2^* of the water signal measured at 9.4 T throughout each study, oxygenation of the brain was always adequate, consistent with the low cerebral lactate, the high glucose content, and the high phosphocreatine content (Fig. 1). The observable tissue glucose resonances measured by ^{1}H NMR spectroscopy (Fig. 1) as well as the high ^{13}C-labeled glucose signal observed by localized ^{13}C NMR in all studies further indicated that substrate delivery to the brain was adequate.

The following four experiments were carried out, some sequentially on the same rat.

Validation of the localization method

A coronal magnetic resonance image of the rat brain with a voxel position indicated by the rectangle is shown in Fig. 2A. Clearly, substantial layers of skeletal muscle tissue ascribed to the temporal jaw muscles can be discerned, and localization of the glycogen signal is therefore necessary.

The pulse sequence developed for three-dimensional localization of the glycogen C1 signal was extensively tested in phantom studies. Using various phantoms mimicking a 1–3-mm-thick muscle layer adjacent to the surface coil, we verified that even when considering three measurements that lasted 3 h each, signal from natural abundance oyster glycogen (400 m*M*) in the outer chamber was suppressed into the spectral noise. Phantom

studies were also used to verify the performance of the localization with respect to voxel definition. The elimination of the phantom glycogen signal implied that a fully labeled muscle glycogen signal corresponding to ~50 m*M* [^{13}C]glycogen would be suppressed to the noise level when measured in 4 min. The observation of a glycogen C1 resonance with a signal-to-noise ratio of ~5:1 measured over 3 min was thus assumed to represent mainly brain glycogen. In addition, when placing the spectrometer frequency at 30.5 ppm to minimize the
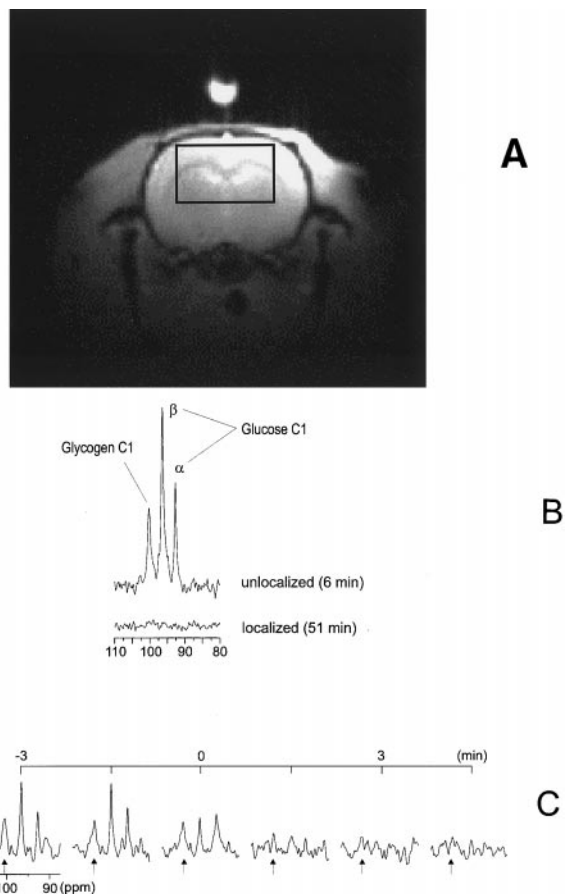

FIG. 2. ^{13}C NMR spectroscopy of rat brain 20 min after cardiac arrest (global ischemia). **A:** A coronal image acquired using the FLASH sequence (*TR* = 10 ms, *TE* = 5 ms). The box indicates the location of the voxel selected (9 × 5.5 mm). The small sphere filled with ^{13}C-labeled formic acid placed at the carbon coil center can be seen at the top. **B:** The top trace shows a spectrum acquired without any localization means. The bottom trace shows a spectrum acquired from a 560-μl volume. The two spectra shown were acquired in an interleaved fashion *simultaneously* over 57 min by alternating blocks of 40-s unlocalized measurements (64 scans) with 5-min blocks of localized measurements (512 scans) and by separately adding the data in the computer. Acquisition was started 20 min after initiating global ischemia. Both spectra were processed with an exponential multiplication (30 Hz line broadening) and are shown without baseline correction. **C:** Horizontal stack plot of localized spectra that were acquired with a 1.5-min temporal resolution from the same rat. KCl was administered at *t* = 0 min. The small arrows indicate the resonance position of glycogen C1 (100.5 ppm). Exponential multiplication (50 Hz line broadening) was applied.
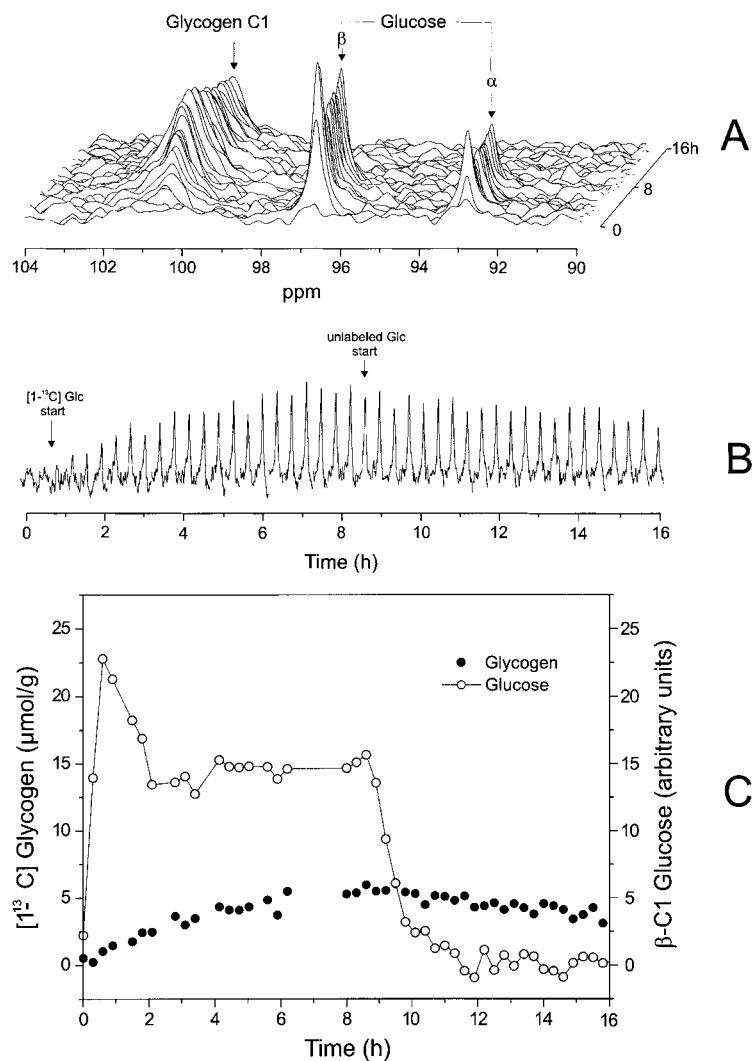
FIG. 3. Time-resolved observation of label incorporation into cerebral brain glycogen. **A:** A stack plot of ^{13}C spectra acquired over a 16-h experiment from one rat. At $t = 0$, the infusion of [1-^{13}C]glucose was started and after 8.5 h (indicated by the arrow) replaced with unlabeled glucose (pulse–chase experiment). Processing consisted of exponential multiplication (30 Hz line broadening), and the spectra are shown without baseline correction. **B:** A horizontal stack plot of the glycogen C1 resonance at 100.5 ppm from the same experiment shown in A. **C:** The corresponding time course of the integrated glycogen C1 resonance (●; left scale) and the integrated β-glucose C1 resonance (○; right scale). The time between 6.5 and 8 h was used for determination of the T_1 of glycogen C1 in vivo and ^{1}H magnetic resonance spectrum collection (similar to Fig. 1). For easier visualization, the spectra used for this plot were pooled to reduce the time resolution to 18 min (by averaging the higher temporal resolution data).

chemical shift displacement error, we noted that even during long accumulations, the intense lipid–$(CH_2)_n$– peak at 30.5 ppm due to the superficial fat was completely suppressed (data not shown), further supporting the accuracy and reliability of the localization method.

To further validate the in vivo localization method, we exploited the difference in agonal breakdown of muscle glycogen (on the order of hours) compared with brain glycogen, which has been reported to be on the order of minutes (Lowry et al., 1964; Swanson et al., 1989). After infusing ^{13}C-labeled glucose for at least 3 h, KCl was administered intravenously to induce cardiac arrest. In spectra collected without the three-dimensional localization method, we consistently observed glycogen and glucose signals, as illustrated in Fig. 2B. The spectra shown in Fig. 2B were acquired over a 57-min period without localization, interleaved with the localization turned on, starting 20 min after intravenous administration of KCl. Without three-dimensional localization of the NMR signals (top), the detected ^{13}C glycogen C1 signal is the sum of the signals originating from the

muscle as well as from the brain. With localization (bottom), this signal completely vanished, confirming that the method efficiently suppresses the noncerebral glycogen C1 signal. Concomitant elimination of the extracerebral glucose signal also indicated adequate localization efficiency for the glucose C1 signals.

Finally, we assessed whether the localized ^{13}C signal was consistent with brain glycogen by measuring the time elapsed until the brain glycogen signal was eliminated after intravenous injection of KCl. These measurements were performed with a 90 s temporal resolution after [1-^{13}C]glucose was infused for at least 4 h ($n = 6$ rats, four of which were part of experimental group II). The glycogen intensity was reduced to 50% of the signal recorded before KCl administration within 1.8 ± 0.1 min (mean $\pm$ SE). After 15 ± 3 min, the glycogen C1 signal was reduced to <10%. Such a rapidly decreasing glycogen signal is illustrated in Fig. 2C. When averaged over all postmortem measurements, the first spectrum acquired after injection of KCl was reduced to $44 \pm 4\%$ (mean $\pm$ SE). The concurrent decrease in ^{13}C-labeled

glucose signal was consistent with that observed by ^1H NMR spectroscopy after KCl administration (authors' unpublished data) and reflect the well-known changes in agonal glucose consumption.

Assessment of rate of ^{13}C incorporation into glycogen C1 (synthase flux)

The duration of [1-^{13}C]glucose infusion, T_{inf}, before continuing the infusion with unlabeled glucose (see experimental group III) was 10 (n = 1 rat), 30 (n = 1), 70 (n = 1), 120 (n = 1), 240 (n = 2), 330 (n = 1), and 550 min (n = 2). All measurements were quantified using the external reference method (based on Eq. 1) just before the end of [^{13}C]glucose infusion. When [1-^{13}C] glucose was infused for at least 30 min, the peak [1-^{13}C]glycogen concentration was 5.1 ± 0.6 μmol g^{-1} glucosyl units (mean ± SE, n = 8 rats).

Label incorporation into glycogen C1 was initially faster and appeared to level off with infusion time, as illustrated in Fig. 3A and B for one rat, for which glucose was infused for 8.5 h. Figure 3C plots the quantified ^{13}C label in glycogen C1 as a function of time after the start of ^{13}C glucose infusion. Good reproducibility was implied by the observation that the *uncorrected* NMR signal from six rats measured with $T_{inf} > 240$ min was highly consistent with a coefficient of interindividual variation of 18% (data not shown).

During the first 60 min of [1-^{13}C]glucose infusion, the rate of ^{13}C-labeled glycogen accumulation assessed as described in Materials and Methods [V_{syn} ($t = 30$) in Fig. 4] was almost fivefold higher (2.3 ± 0.7 μmol g^{-1} h^{-1}; n = 9) and remained higher for the first 90 min ($p < 0.01$) than that measured ≥2 h after the start of the infusion (0.49 ± 0.14 μmol g^{-1} h^{-1}), indicated by V_{syn} ($t > 150$) in Fig. 4. The 24 measurements that were used for calculating V_{syn} ($t > 150$) did not show a correlation with time as judged from the low correlation coefficient ($r = -0.04$, $p > 0.05$).

Assessment of [1-^{13}C]glycogen decrease during unlabeled glucose infusions (phosphorylase flux)

To determine whether the change in the apparent rate of [1-^{13}C]glycogen accumulation such as the one shown in Fig. 3 can be ascribed entirely to turnover (when brain glycogen synthesis and breakdown rates are similar), we switched the infusate to unlabeled glucose after T_{inf} minutes (n = 7 rats). This was done with the same infusion protocol (but by switching from labeled to unlabeled glucose) in all of the experiments described in Assessment of rate of ^{13}C incorporation into glycogen C1 (synthase flux), except for three cases (n = 6). In an additional study, ^{13}C-labeled glucose was infused for only 3 min (half-bolus) (n = 1). The rate of glycogen C1 decrease, denoted V_{phos}, was measured as described in Materials and Methods for at least the following 3 h. In these experiments, the simultaneously detected, localized glucose signals were reduced to <10% of the initial value within 2 h after the start of the unlabeled glucose infusion. When the glucose signals were no longer de-
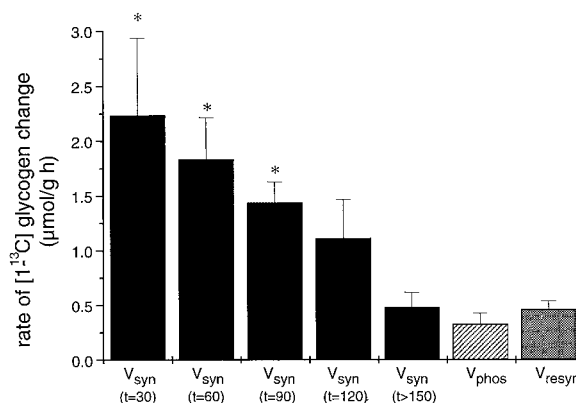

FIG. 4. Rate of brain [1-^{13}C]glycogen changes during glucose infusions. The solid columns indicate the rate of glycogen signal change (determined by calculating the slope of a linear regression over a 60-min interval, as described in Materials and Methods) during infusion of [1-^{13}C]glucose (V_{syn}), measured at $t = 30$ (n = 9 measurements from n = 9 rats), 60 (n = 9), 90 (n = 9), and 120 min (n = 9). The fifth column indicates V_{syn} measured at $t > 150$ min (n = 24 measurements). The hatched column (phosphorylase flux, V_{phos}) indicates the rate of [1-^{13}C]glycogen decrease after the infusion was changed to unlabeled glucose (n = 39, experimental group III) in seven rats. The stippled column indicates the rate of [1-^{13}C]glycogen increase, V_{resyn}, after prolonged periods of unlabeled glucose infusions (n = 20 from three rats, experimental group IV). Data are mean ± SE (bars) values. *$p < 0.01$ with a two-tailed t test versus V_{syn} ($t > 150$).

tectable by localized in vivo NMR, the brain glycogen signal was 80 ± 4% of the maximum, suggesting that glycogen was still highly enriched with ^{13}C-labeled glucosyl units. During further infusion of unlabeled glucose, the glycogen C1 signal remained remarkably stable, as can also be seen from the stack plot (Fig. 3A). The glycogen C1 resonance is shown in the horizontal stack plot (Fig. 3B), and the time course of the integrated resonance is plotted in Fig. 3C. The average rate of [1-^{13}C]glycogen decrease during natural abundance glucose infusions was 0.33 ± 0.10 μmol g^{-1} h^{-1} (mean ± SE). Because the change in the glycogen signal was assessed over intervals of 60 min each, the extended times that were measured in the seven rats resulted in 39 rate assessments. Pooling the measurements of glycogen decrease during the first 120 min after starting the unlabeled glucose infusion into one data set (n = 18 rate assessments) and the remaining measurements into a second measurement (n = 21) showed that the rates were not different (0.38 ± 0.19 vs. 0.29 ± 0.09 μmol g^{-1} h^{-1}, respectively; $p > 0.05$). The rate of glycogen degradation was also independent of the duration of the preceding infusion of labeled glucose, T_{inf} ($r = 0.25$, $p > 0.05$), e.g., even when infusing only the first half of the bolus (0.12 g of glucose per rat), the brain [1-^{13}C]glycogen concentration of 0.25 μmol g^{-1} resulted in a signal that was detectable 30 min after the start of the glucose infusion and that remained detectable for >2 h. Likewise, when the glucose infusion was switched from ^{13}C-labeled to unlabeled glucose after 10 min (0.2 g of

glucose per rat), [1-^{13}C]glycogen increased to 0.55 μmol g^{-1}, which remained detectable for the next 4 h. V_{phos} did not show a correlation with T_{inf} ($r = -0.25$, $p > 0.05$).

Assessment of [1-^{13}C]glycogen accumulation after preceding hyperglycemia

To ascertain the degree by which the ^{13}C label incorporation curves might reflect glycogen turnover rather than net glycogen accumulation, we started the infusion using the same infusion protocol in three rats, by first infusing unlabeled glucose for at least 4 h, which was then switched to [1-^{13}C]glucose, and the rate of [1-^{13}C]-glycogen synthesis after preceding unlabeled glucose infusion (V_{resyn}) was measured as described in Materials and Methods. The rate of brain [1-^{13}C]glycogen accumulation was measured over at least 3 h, resulting in n = 20 rate assessments, from which V_{resyn} in Fig. 4 was calculated at 0.46 $\pm$ 0.08 μmol g^{-1} h^{-1} (mean $\pm$ SE). This rate of [^{13}C]glycogen accumulation after prolonged hyperglycemia did not show a correlation with time ($r = 0.15$, $p > 0.05$ for correlation).

DISCUSSION

Validation of the localization method

The rapid decrease of ^{13}C-labeled glycogen C1 signal observed postmortem (Fig. 2C) was consistent with the majority of the localized signal being in vivo from brain glycogen, because postmortem muscle glycogenolysis is much slower. The rate of ^{13}C-labeled glucose decrease was as fast and consistent with ^{1}H observations of the total glucose content (authors' unpublished data). We observed a slightly slower rate of glycogen degradation during global ischemia than what has been reported (Lowry et al., 1964; Swanson et al., 1989). However, the first spectrum acquired after injection of KCl was reduced to 44% of the initial value, ruling out major contributions from muscle glycogen to the signal. A factor that might have contributed to the slightly slower rate of brain glycogen breakdown was the finite time of 1–2 min that elapsed between injection of KCl and complete global brain ischemia.

Quantification of ^{13}C-labeled glycogen C1 accumulation

Published literature values for total glycogen content in the rat cortex range between 2 and 6 μmol g^{-1} glucosyl units, assuming 12.5% protein content in brain (Strang and Bachelard, 1971; Sagar et al., 1987; Garriga and Cusso, 1992). The 5.1 μmol g^{-1} ^{13}C-labeled brain glycogen C1 observed after several hours is consistent with these published values. However, under conditions of infusing ^{13}C-labeled glucose, the measured ^{13}C label in glycogen only represents total glycogen content if net synthesis or breakdown is 0 and all glucosyl units have been turned over. This may not be the case during hyperglycemia, which has been shown to lead to modest increases in brain glycogen content, and concentrations approaching 10 μmol g^{-1} have been reported in the rat

brain (Nelson et al., 1968). Assuming a turnover rate of 0.5 $\pm$ 0.14 μmol g^{-1} h^{-1} based on the values of V_{syn} ($t > 150$) shown in Fig. 4, label incorporation due to turnover was estimated to be 2.0 $\pm$ 0.6 μmol g^{-1} over 4 h, and net glycogen synthesis was estimated at 3.1 $\pm$ 0.8 μmol g^{-1}. When assuming a glycogen concentration of ~5 μmol g^{-1} (Sagar et al., 1987), a modest 60% increase in brain glycogen is calculated, which is in good agreement with the observations in unanesthetized brain reported by Nelson et al. (1968).

Assessment of glycogen turnover rates during glucose infusions

The rate of ^{13}C incorporation into glycogen C1 was initially higher and decreased with T_{inf}. In contrast, the rate of ^{13}C-labeled glycogen C1 decrease (V_{phos} in Fig. 4) during subsequent unlabeled glucose infusions did not correlate with the duration of the unlabeled glucose infusion or the duration of the preceding [^{13}C]glucose infusion. Because the label washout from glycogen was (a) very slow and (b) not a function of time or of the time of the preceding labeled glucose infusion, an initial rate was observed. This supports our assertion that after prolonged glucose infusions, glycogen turnover is very slow. The rapid initial label incorporation is consistent with a study showing rapid activation of synthase and inactivation of phosphorylase after glucose loading (Cummins et al., 1983). The stability of the glycogen C1 signal implied that brain glycogen turnover was slow (~0.5 μmol g^{-1} h^{-1}), and V_{syn} ($t > 150$) ~ V_{phos} ~ V_{resyn} (Fig. 4) implied that net glycogen synthesis was minimal after a few hours. The glycogen turnover rates and the initial glycogen C1 synthesis rates observed in this study were on the order of 30–150 times slower than the rate of glucose consumption of ~0.8 μmol g^{-1} min^{-1} in the resting rat brain (Ueki et al., 1992) and imply a stable brain glycogen pool in the *unstimulated,* lightly anesthetized rat brain during glucose infusions.

A potential confounding factor can be the rate of change in the fractional enrichment of the precursor glucose being different between the initial [^{13}C]glucose administration and the subsequent unlabeled glucose infusion. These differences were estimated to have a negligible impact on these calculations of rate changes, because the rate of glucose disappearance after switching to unlabeled glucose infusions was fast compared with the rate of glycogen breakdown: When the glucose signals were no longer detectable by localized in vivo NMR, the brain glycogen signal was still 80% of the peak observed ^{13}C concentration, suggesting that glycogen was still highly enriched with ^{13}C-labeled glucosyl units. The labeled glycogen pool should decrease with ~0.8 V_{syn} ($t = 30$), if $V_{syn} = V_{phos}$, which was clearly not the case for brain glycogen in the present study, which suggests that although turnover on the order of 0.5 μmol g^{-1} h^{-1} was present, it was slow and unlikely to account completely for the rapid initial rise in brain [1-^{13}C]glycogen.

Incorporation of deoxyglucose into brain glycogen 45 min after a pulse of ^{14}C-labeled deoxyglucose has been assessed to contain 2% of total tissue radioactivity, with the majority of label trapped in the nonmetabolizable 2-deoxyglucose-6-phosphate (Nelson et al., 1984). Our results support the notion that short administrations of labeled glucose lead to minor amounts of the label incorporated into brain glycogen.

The hyperglycemia present in our experiment most likely resulted in concomitant hyperinsulinemia, which results in profound glycogen accumulation in astrocyte cultures (Swanson and Choi, 1993, and references therein).

To what extent the activity of gluconeogenesis reported in astrocyte cultures (Schmoll et al., 1995) is also present in vivo remains to be determined. In our experiments, label scrambling at the triose phosphate level (from the C1 to the C6 position and vice versa) leads to an underestimation of the rate of glycogen synthesis.

We conclude that intravenous [^{13}C]glucose infusion results in a slow but efficient labeling of the astrocytic glycogen. The new, completely noninvasive NMR methods we have developed for this purpose can be readily extended to study human brain glycogen metabolism, which should lead to a much-improved understanding of the regulation of cerebral glycogen metabolism at rest during hypoglycemia and during functional activation.

REFERENCES

Adriany G. and Gruetter R. (1997) A half volume coil for efficient proton decoupling in humans at 4 Tesla. *J. Magn. Reson.* **125,** 178–184.

Chee N. P., Geddes R., and Wills P. R. (1983) Metabolic heterogeneity in rabbit brain glycogen. *Biochim. Biophys. Acta* **756,** 9–12.

Chen W., Avison M. J., Bloch G., and Shulman R. G. (1994) Proton NMR observation of glycogen in vivo. *Magn. Reson. Med.* **31,** 576–579.

Chen Y. J., Rachamadugu S., and Fernandez E. J. (1997) Three dimensional outer volume suppression for short echo time in vivo ^{1}H spectroscopic imaging in rat brain. *Magn. Reson. Imaging* **15,** 839–845.

Cummins C. J., Lust W. D., and Passonneau J. V. (1983) Regulation of glycogen metabolism in primary and transformed astrocytes *in vitro. J. Neurochem.* **40,** 128–136.

Fitzpatrick S. M., Hetherington H. P., Behar K. L., and Shulman R. G. (1990) The flux from glucose to glutamate in the rat brain in vivo as determined by ^{1}H-observed, ^{13}C-edited NMR spectroscopy. *J. Cereb. Blood Flow Metab.* **10,** 170–179.

Folbergrová J., Katsura K. I., and Siesjö B. K. (1996) Glycogen accumulated in the brain following insults is not degraded during a subsequent period of ischemia. *J. Neurol. Sci.* **137,** 7–13.

Garriga J. and Cusso R. (1992) Effect of starvation on glycogen and glucose metabolism in different areas of the rat brain. *Brain Res.* **591,** 277–282.

Gruetter R. (1993) Automatic, localized in vivo adjustment of all first- and second-order shim coils. *Magn. Reson. Med.* **29,** 804–811.

Gruetter R., Prolla T. A., and Shulman R. G. (1991) ^{13}C-NMR visibility of rabbit muscle glycogen in vivo. *Magn. Reson. Med.* **20,** 327–332.

Gruetter R., Magnusson I., Rothman D. L., Avison M. J., Shulman R. G., and Shulman G. I. (1994*a*) Validation of ^{13}C NMR measurements of liver glycogen in vivo. *Magn. Reson. Med.* **31,** 583–588.

Gruetter R., Novotny E. J., Boulware S. D., Mason G. F., Rothman D. L., Shulman G. I., Prichard J. W., and Shulman R. G. (1994*b*) Localized ^{13}C NMR spectroscopy in the human brain of amino acid labeling from D-[1-^{13}C]glucose. *J. Neurochem.* **63,** 1377–1385.

Gruetter R., Seaquist E., Kim S.-W., and Ugurbil K. (1998*a*) Localized *in vivo* ^{13}C NMR of glutamate metabolism. Initial results at 4 Tesla. *Dev. Neurosci.* **20,** 380–388.

Gruetter R., Weisdorf S. A., Rajanayagan V., Terpstra M., Merkle H., Truwit C. L., Garwood M., Nyberg S. L., and Ugurbil K. (1998*b*) Resolution improvements in in vivo ^{1}H NMR spectra with increased magnetic field strength. *J. Magn. Reson.* **135,** 260–264.

Lowry O., Passonneau J., Hasselberger F., and Schulz D. (1964) Effect of ischemia on known substrates and cofactors of the glycolytic pathway in brain. *J. Biol. Chem.* **239,** 18–30.

Luo Y., Tannus A., and Garwood M. (1995) Frequency-selective elimination of coherent signal with B1 insensitivity: an improved outer-volume suppression method (BISTRO), in *3rd Scientific Meeting of the Society of Magnetic Resonance,* p. 1017. Society for Magnetic Resonance, Nice, France.

Magistretti P. J., Hof P. R., and Martin J. L. (1986) Adenosine stimulates glycogenolysis in mouse cerebral cortex: a possible coupling mechanism between neuronal activity and energy metabolism. *J. Neurosci.* **6,** 2558–2562.

Meguid M. M., Beverly J. L., Yang Z. J., Gleason J. R., Meguid R. A., and Yue M. X. (1993) Parenteral nutrition, brain glycogen, and food intake. *Am. J. Physiol.* **265,** R1387–R1391.

Nelson S. R., Schulz D. W., Passonneau J. V., and Lowry O. H. (1968) Control of glycogen levels in brain. *J. Neurochem.* **15,** 1271–1279.

Nelson T., Kaufman E. E., and Sokoloff L. (1984) 2-Deoxyglucose incorporation into rat brain glycogen during measurement of local cerebral glucose utilization by the 2-deoxyglucose method. *J. Neurochem.* **43,** 949–956.

Newgard C. B., Littman D. R., van Genderen C., Smith M., and Fletterick R. J. (1988) Human brain glycogen phosphorylase. Cloning, sequence analysis, chromosomal mapping, tissue expression, and comparison with the human liver and muscle isozymes. *J. Biol. Chem.* **263,** 3850–3857.

Ordidge R. J., Connelly A., and Lohman J. A. B. (1986) Image-selected in vivo spectroscopy (ISIS). A new technique for spatially selective NMR spectroscopy. *J. Magn. Reson.* **66,** 283–294.

Overloop K., Vanstapel F., and Vanhecke P. (1996) C-13-NMR relaxation in glycogen. *Magn. Reson. Med.* **36,** 45–51.

Patlak C. S. and Pettigrew K. D. (1976) A method to obtain infusion schedules for prescribed blood concentration time courses. *J. Appl. Physiol.* **40,** 458–463.

Pellegri G., Rossier C., Magistretti P. J., and Martin J. L. (1996) Cloning, localization and induction of mouse brain glycogen synthase. *Brain Res. Mol. Brain Res.* **38,** 191–199.

Pfeiffer B., Meyermann R., and Hamprecht B. (1992) Immunohistochemical co-localization of glycogen phosphorylase with the astroglial markers glial fibrillary acidic protein and S-100 protein in rat brain sections. *Histochemistry* **97,** 405–412.

Sagar S. M., Sharp F. R., and Swanson R. A. (1987) The regional distribution of glycogen in rat brain fixed by microwave irradiation. *Brain Res.* **417,** 172–174.

Salvan A. M., Vion-Dury J., Confort-Gouny S., Dano P., and Cozzone P. J. (1997) Increased cerebral glycogen detected by localized

[1]H-magnetic resonance spectroscopy in a patient with suspected McArdle's disease. *Eur. Neurol.* **37,** 251–253.

Schmoll D., Fuhrmann E., Gebhardt R., and Hamprecht B. (1995) Significant amounts of glycogen are synthesized from 3-carbon compounds in astroglial primary cultures from mice with participation of the mitochondrial phosphoenolpyruvate carboxykinase isoenzyme. *Eur. J. Biochem.* **227,** 308–315.

Shaka A. J., Keeler J., and Freeman R. (1983) Evaluation of a new broadband decoupling sequence: WALTZ-16. *J. Magn. Reson.* **53,** 313–340.

Shulman R. G., Bloch G., and Rothman D. L. (1995) In vivo regulation of muscle glycogen synthase and the control of glycogen synthesis. *Proc. Natl. Acad. Sci. USA* **92,** 8535–8542.

Shungu D. C. and Glickson J. D. (1993) Sensitivity and localization enhancement in multinuclear in vivo NMR spectroscopy by outer volume presaturation. *Magn. Reson. Med.* **30,** 661–671.

Siesjö B. (1978) *Brain Energy Metabolism,* pp. 101–110. Wiley, New York.

Sorg O. and Magistretti P. J. (1992) Vasoactive intestinal peptide and noradrenaline exert long-term control on glycogen levels in astrocytes: blockade by protein synthesis inhibition. *J. Neurosci.* **12,** 4923–4931.

Strang R. H. and Bachelard H. S. (1971) Extraction, purification, and turnover of rat brain glycogen. *J. Neurochem.* **18,** 1067–1076.

Swanson R. A. (1992) Physiologic coupling of glial glycogen metabolism to neuronal activity in brain. *Can. J. Physiol. Pharmacol.* **70** (Suppl.), S138–S144.

Swanson R. A. and Choi D. W. (1993) Glial glycogen stores affect neuronal survival during glucose deprivation in vitro. *J. Cereb. Blood Flow Metab.* **13,** 162–169.

Swanson R. A., Sagar S. M., and Sharp F. R. (1989) Regional brain glycogen stores and metabolism during complete global ischaemia. *Neurol. Res.* **11,** 24–28.

Swanson R. A., Morton M. M., Sagar S. M., and Sharp F. R. (1992) Sensory stimulation induces local cerebral glycogenolysis: demonstration by autoradiography. *Neuroscience* **51,** 451–461.

Tannus A. and Garwood M. (1996) Improved performance of frequency-swept pulses using offset-independent adiabaticity. *J. Magn. Reson. A* **120,** 133–137.

Taylor R., Price T. B., Rothman D. L., Shulman R. G., and Shulman G. I. (1992) Validation of ^{13}C NMR measurement of human skeletal muscle glycogen by direct biochemical assay of needle biopsy samples. *Magn. Reson. Med.* **27,** 13–20.

Terpstra M., Gruetter R., High W. B., Mescher M., DelaBarre L., Merkle H., and Garwood M. (1998) Lactate turnover in rat glioma measured by in vivo nuclear magnetic resonance spectroscopy. *Cancer Res.* **58,** 5083–5088.

Tkac I., Starcuk Z., Choi I.-Y., and Gruetter R. (1999) In vivo ^{1}H NMR spectroscopy of rat brain at 1 ms echo time. *Magn. Reson. Med.* **41,** 649–656.

Ueki M., Mies G., and Hossmann K. A. (1992) Effect of alpha-chloralose, halothane, pentobarbital and nitrous oxide anesthesia on metabolic coupling in somatosensory cortex of rat. *Acta Anaesthesiol. Scand.* **36,** 318–322.

Wiesinger H., Hamprecht B., and Dringen R. (1997) Metabolic pathways for glucose in astrocytes. *Glia* **21,** 22–34.

Zang L. H., Laughlin M. R., Rothman D. L., and Shulman R. G. (1990) 13C NMR relaxation times of hepatic glycogen in vitro and in vivo. *Biochemistry* **29,** 6815–6820.